Structural analysis of pressure-amorphized zirconium tungstate

A. K. Arora,[1,*] Taku Okada,[2] and Takehiko Yagi[2]
[1]*Condensed Matter Physics Division, Indira Gandhi Centre for Atomic Research, Kalpakkam 603102, India*
[2]*Institute for Solid State Physics, The University of Tokyo, Kashiwanoha 5-1-5, Kashiwa, Chiba 277-8581, Japan*
(Received 10 June 2009; revised manuscript received 1 February 2010; published 6 April 2010)

The negative thermal-expansion material zirconium tungstate, when subjected to a moderate pressure of 2 GPa, turns amorphous irreversibly; the amorphous state being ~26% more dense than the crystalline phase α-$Zr(WO_4)_2$. Structure of pressure-amorphized $Zr(WO_4)_2$ is investigated using synchrotron x-ray diffraction. Structure factors $S(q)$ of samples recovered from different pressures are obtained. The first peak in $S(q)$ for 10.5 GPa-treated sample is found to occur at a slightly larger q than that recovered from 5.5 GPa, suggesting that the amorphous samples recovered from higher pressure could be more dense. The pair-correlation functions $g(r)$, obtained by Fourier transforming $S(q)$, suggests that the further densification of amorphous phase occurs via contraction of second and third neighbor shells representing O-O and W-W and W-Zr distances rather than first neighbor shell. In contrast to earlier speculations, the present results do not show evidence for an increase in the coordination number and consequent existence of distinct amorphous phases in samples recovered from pressures up to 10.5 GPa.

DOI: 10.1103/PhysRevB.81.134103 PACS number(s): 61.43.Er, 64.70.K−, 64.60.−i

I. INTRODUCTION

There is considerable current interest in materials that exhibit negative thermal expansion (NTE) (Refs. 1–4) from the point of view of understanding the mechanism.[5–7] In addition, these materials are useful for synthesizing composites and solid solutions with desired coefficient of thermal expansion including zero thermal expansion.[8–10] Among the NTE materials, zirconium tungstate is of special interest because of large isotropic negative coefficient of expansion over a wide temperature range. Consequently numerous investigations using a variety of techniques have been carried out to probe various physical properties[11–18] including phase transitions driven by temperature[3,19,20] and pressure.[21–23] The ambient temperature cubic (α) phase of $Zr(WO_4)_2$ consists of a corner-linked network of WO_4 and ZrO_6 polyhedra. $Zr(WO_4)_2$ and several other compounds with similar network structures are found to turn amorphous at high pressure[11,24,25] and the amorphization is often irreversible. The amorphous zirconium tungstate a-$Zr(WO_4)_2$ recovered after releasing the pressure is found to be substantially denser than the starting cubic α phase.[26] The density, structure, and stability of a-$Zr(WO_4)_2$ has been studied by several investigators[26–33] and the samples are found to recrystallize to the α phase when annealed above 900 K. On the other hand, if a-$Zr(WO_4)_2$ is heated while under high pressure, it is reported to either decompose into mixture of simple oxides[30] or go to hexagonal U_3O_8-type structure[31] depending on the pressure and temperature of the treatment. The specific volumes (volume per formula unit) of a-$Zr(WO_4)_2$ recovered after pressure cycling in large-volume piston-cylinder-type high-pressure apparatuses ranged between 142.6 and 152.6 Å^3 for samples treated between 4 and 7.5 GPa. The diffraction pattern of a-$Zr(WO_4)_2$ recovered from 4 GPa has been fitted to an amorphous structure with oxygen coordination of tungsten to be 5. In addition, an increase in the coordination number of Zr to 7 has also been recently found in a-$Zr(WO_4)_2$ from Zr K-edge extended x-ray-absorption fine structure.[32] Whereas the oxygen coordination of W and Zr in the cubic phase are 4 and 6, respectively. Earlier a sixfold coordinated structure as a precursor to decomposition into a mixture of simple oxides has also been suggested.[26] Decomposition of network structures subsequent to pressure-induced amorphization into mixtures of simple oxides has indeed been found to occur at ambient temperature in ZrV_2O_7 (Ref. 25) and at elevated temperature in $Zr(WO_4)_2$.[30] Formation of a sevenfold coordinated amorphous phase with short-range order analogous to hexagonal U_3O_8-type structure could also occur at higher pressures.[31] This suggests that there are several possibilities for the amorphous phase in terms of coordination numbers. The reported different densities of recovered samples and higher coordination numbers raise the question whether this could be due to polyamorphism[34] (distinct amorphous states) similar to that reported in ice,[35] a-Si,[36] and fused quartz.[37] In order to explore this possibility, it is important to reinvestigate the amorphous phase recovered from different pressures using a single apparatus and see if there exist any systematic differences in the structure. In the present work, we have investigated the structure of pressure-amorphized $Zr(WO_4)_2$ using synchrotron radiation at Photon Factory. The a-$Zr(WO_4)_2$ samples were prepared by pressure-cycling cubic $Zr(WO_4)_2$ to different pressures in a gasketed diamond-anvil cell (DAC). The scattered intensity was analyzed to obtain the structure factor $S(q)$, which was Fourier transformed to give the pair-correlation function $g(r)$. The changes in $S(q)$ and $g(r)$ are discussed in the context of the possibility of polyamorphism.

II. EXPERIMENTAL DETAILS

Zirconium-tungstate samples used in the present experiments were synthesized by Dr. T. A. Mary. Each powdered sample was loaded into a 300 micron hole, drilled through a preindented stainless-steel gasket (about 70 μm thick) of a Mao-Bell-type high-pressure diamond-anvil cell. No

pressure-transmitting medium was used in the DAC. Ruby fluorescence was used for the estimation of pressure. Samples were soaked at the desired pressure for 2 h and then the pressure was released. Although amorphization is reported to occur at 2.1 GPa,[11] it is likely that amorphization may not be complete by this pressure. In view of this the pressure soaking was done at 5.5, 7.5, and 10.5 GPa. The recovered gaskets, with the sample embedded in the gasket hole, were used as such in the x-ray diffraction measurements that were made using synchrotron radiation [$\lambda = 0.4270(2)$ Å] from 13A beamline at Photon Factory, KEK. A 30 μm collimator was used and an xy translation stage was used for aligning the sample in the hole of the gasket with the collimator. An image plate was used as the detector. The two-dimensional (2D) image plate data were integrated to convert it to one-dimensional intensity versus 2θ data. An image plate distance of 344.6(1) mm from the sample permitted a maximum scattering angle 2θ of 32.52°. Air-scattering data were collected without the sample in a separate experiment. Transmittances of the direct beam through the samples were also measured.

III. DATA ANALYSES AND RESULTS

Figure 1(a) shows the as-measured data as a function of scattering angle 2θ. One can see typical amorphouslike scattering pattern for all the samples. Weaker scattering pattern for 10.5 GPa sample is due to smaller sample thickness. In 5.5 GPa sample, four weak sharp diffraction peaks at 6.15°, 6.82°, 7.73°, and 9.12° 2θ riding over the first amorphous peak correspond to the high-pressure orthorhombic γ-$Zr(WO_4)_2$ phase and imply persistence of a few small crystalline grains in the amorphous phase. A comparison of the intensity of these weak peaks with those of a fully crystalline sample suggests that the residual crystalline fraction is less than 0.1%. One can see from the 2D image of the scattering pattern [inset in Fig. 1(a)] that only a few weak diffraction spots are present. 7.5 GPa sample shows only one weak sharp diffraction peak. In order to remove the weak diffraction peaks riding over the amorphous scattering pattern, the data were filtered using OMITSPOT software. Figure 1(b) shows the resulting patterns. One can see that the intensities of the diffraction peaks have substantially reduced; however, these could not be completely eliminated. For more detailed quantitative analysis, the OMITSPOT data were used.

One can see from Fig. 1 that the scattering patterns ride on a rising background toward lower 2θ. This background arises due to air scattering. In order to quantitatively estimate the contribution of air scattering to the background, air scattering was measured in a separate experiment and is shown as inset in Fig. 1(b). The air-scattering data were used as such, after suitable scaling, for subtracting the background. The measured x-ray scattering intensity was analyzed after applying corrections for air scattering and attenuation in the samples using the following procedure. The corrected intensity $I^{cor}(q)$ is obtained as

$$I^{cor}(q) = \left[\frac{I^{obs}(q)}{I_0} - \frac{I^{air}(q)}{I_0'}\exp(-\mu t)\right]\frac{1}{F(\mu t, 2\theta)}, \quad (1)$$

where $q = 4\pi\lambda^{-1}\sin\theta$ is the scattering vector and $I^{obs}(q)$ is the measured scattered intensity at the incident-beam intensity I_0. The intensity arising from the air scattering $I^{air}(q)$, measured at incident intensity I_0', is also normalized to unit incident intensity. Normalization of intensities by I_0 and I_0' is required to account for change in the synchrotron intensity (current) between different experiments. As only the transmitted intensity through the sample contributes to the air scattering, the second term is multiplied by the transmission factor of the direct beam, i.e., $\exp(-\mu t)$, where μ is the linear absorption coefficient and t the sample thickness. $F(\mu t, 2\theta)$ is the correction factor for the angle-dependent attenuation in the sample given as

$$F(\mu t, 2\theta) = [1 - \exp\{-\mu t(\sec 2\theta - 1)\}]/[\mu t(\sec 2\theta - 1)]. \quad (2)$$

One can see that $F(\mu t, 2\theta) \to 1$ if $\theta \to 0$ or $t \to 0$ or $\mu \to 0$. Figure 2 shows the corrected intensity along with the intensity before applying the $F(\mu t, 2\theta)$ correction for the 7.5 GPa sample. One can see that in the present strongly absorbing a-$Zr(WO_4)_2$ sample $F(\mu t, 2\theta)$ correction significantly modifies intensity at large q.

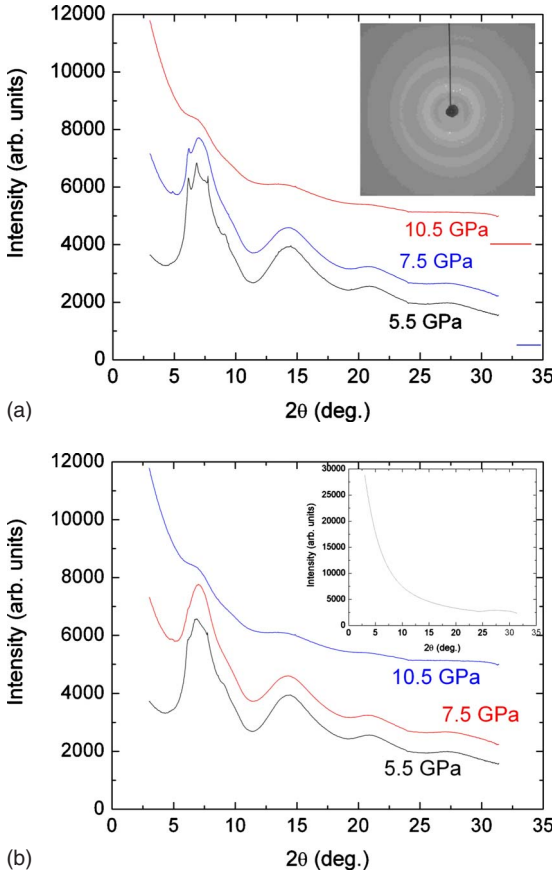

FIG. 1. (Color online) (a) Observed scattered intensity as a function of scattering angle at ambient for a-$Zr(WO_4)_2$ samples recovered from different pressures. The curves are shifted vertically for the sake of clarity. The inset shows the 2D scattering pattern of 5.5 GPa-treated sample containing a few diffraction spots. (b) The scattering data were filtered through OMITSPOT program. The inset shows the air-scattering data recorded without the sample in the path of the beam.

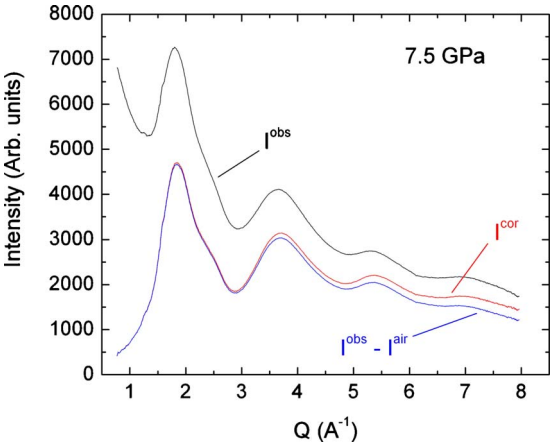

FIG. 2. (Color online) The OMITSPOT intensity before and after subtracting air-scattering background for 7.5 GPa sample. The corrected intensity $I^{cor}(q)$ after implementing correction for angle-dependent attenuation is also shown.

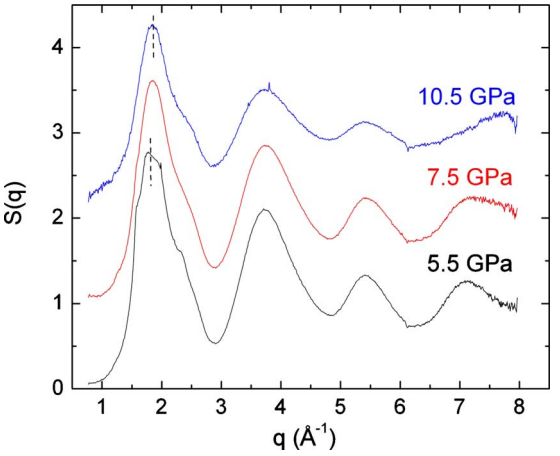

FIG. 3. (Color online) Structure factors for a-$Zr(WO_4)_2$ recovered from different pressures. The curves are vertically displaced for the sake of clarity. Dashed vertical lines represent the peak centers. Note that the height of the first peak reduces as the soaking pressure increases.

The coherent scattering $I^{coh}(q)$ was obtained by multiplying the corrected intensity by a normalization constant α/n_0N and subtracting the incoherent scattering $\langle I^{incoh}(q)\rangle$ arising from Compton background as

$$I^{coh}(q) = (\alpha/n_0N)I^{cor}(q) - \langle I^{incoh}(q)\rangle, \tag{3}$$

where n_0 is the total number of atoms in the compound (11 for ZrW_2O_8) and N is the number of formula units per unit cell. The normalization constant α/n_0N is obtained from the total scattered intensity using Krogh-Moe method[38] as

$$\alpha\int I^{cor}(q)q^2dq = n_0N\left\{\int \langle f^2(q)\rangle q^2dq + \int \langle I^{incoh}(q)\rangle q^2dq - 2\pi^2\langle Z^2\rangle\right\}, \tag{4}$$

where $\langle Z^2\rangle$ is the mean-square atomic number. $\langle Z^2\rangle = (\Sigma_j n_j Z_j^2)/n_0$, where n_j is number of jth-type atom of atomic number Z_j in the compound ($\Sigma_j n_j = n_0$). Similarly averaged $\langle f^2(q)\rangle$ and $\langle I^{incoh}(q)\rangle$ are, respectively, defined as $\langle f^2(q)\rangle = [\Sigma_j n_j f_j^2(q)]/n_0$ and $\langle I^{incoh}(q)\rangle = [\Sigma_j n_j I_j^{incoh}(q)]/n_0$. $f_j(q)$ and $I_j^{incoh}(q)$ are, respectively, the atomic form factor and incoherent scattering from the jth-type atom in the compound. $I_j^{incoh}(q)$ can be theoretically calculated from the reported[39] analytic approximation. Similarly $f_j(q)$ are also obtainable from nine-parameter analytic expressions[40] for the atomic form factors. Thus all the terms on the right-hand side of Eq. (4) are theoretically calculated while the term on the left-hand side is obtained from the experimental data. The normalization constant α/n_0N is thus obtained by taking the appropriate ratio. The structure factor $S(q)$ is then calculated[41] from the coherent scattering as

$$S(q) = 1 + \frac{I^{coh}(q)}{\langle f(q)\rangle^2} - \frac{\langle f^2(q)\rangle}{\langle f(q)\rangle^2}, \tag{5}$$

where $\langle f(q)\rangle = [\Sigma_j n_j f_j(q)]/n_0$. Figure 3 shows the structure factors of amorphous zirconium tungstate recovered from different pressures. The $S(q)$ of 5.5 GPa treated sample is similar to that reported[28] for a-$Zr(WO_4)_2$ recovered from 4 GPa; however, the pressure dependence had not been investigated earlier.

IV. DISCUSSIONS

The broad peaks in the structure factor of amorphous solids and liquids arise from short- and medium-range structural correlations. The systematic changes in the height and the position of the first broad peak have been often analyzed to obtain insight about evolution of the structural correlations[42,43] and relative density.[44,45] One can see from Fig. 3 that the height of the first peak and subsequent oscillations around $S(q)=1$ decrease for samples recovered from successively higher pressures, This suggests that the structural correlations within the amorphous state become weaker as the amorphous samples are subjected to higher pressures. The position of the first peak q_P in the $S(q)$ is known to be inversely correlated with the nearest-neighbor distance and shifts to higher values at higher densities when the system is subjected to high pressure. This is in analogy with the shift of diffraction peaks arising from reflections from unique $(h\ k\ l)$ planes in crystalline solids at high pressure. The present diffraction patterns (Fig. 3) suggest that the first peak in 10.5 GPa-treated sample is centered at slightly larger q than that in the 5.5 GPa sample. This suggests that the density of 10.5 GPa-treated sample could be higher than that of the 5.5 GPa sample.

In order to compare the structures of the amorphous phases in the real space, the structure factor was Fourier transformed using MATLAB to obtain the pair-correlation function $g(r)$ using following equation:

$$g(r) = 1 + \frac{1}{2\pi^2 r n_0 N}\int [S(q) - 1]q\sin(qr)dq. \tag{6}$$

Figure 4 shows the pair-correlation functions for the three recovered samples. As the $S(q)$ data are available only up to

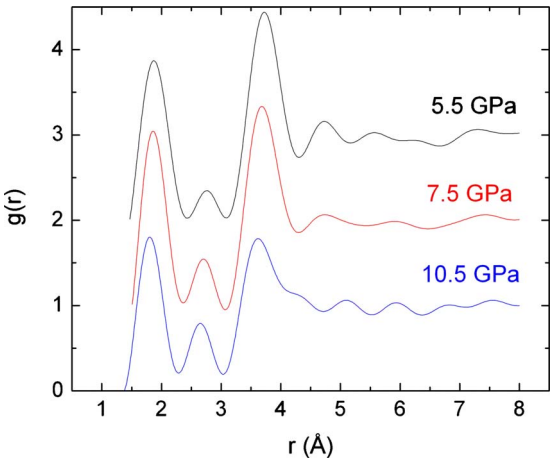

FIG. 4. (Color online) Pair-correlation function $g(r)$ obtained by Fourier transforming the structure factor. Curves are shifted vertically for the sake of clarity.

certain q, the range of integration becomes finite. This is known to result in spurious high-frequency oscillations[44] in the calculated $g(r)$. For avoiding such spurious oscillations, often Blackman[44] or Sinc[41] windows are employed for integration. In order to ascertain the possible existence of such spurious oscillations in $g(r)$ obtained from the present analysis, $g(r)$ was also calculated using a Sinc window. This was found to reduce only the amplitude of peaks in $g(r)$ whereas no peaks were found to disappear confirming that all the features were genuine. In view of this $g(r)$ obtained without using any window was used for further analysis. The three prominent peaks in $g(r)$ in Fig. 4 are qualitatively similar to those reported[28] for a-$Zr(WO_4)_2$ recovered from 4 GPa. One can see that the first peak in $g(r)$ appears at 1.88 Å in the 5.5 GPa-treated sample and marginally shifts to the left at higher pressures. On the other hand, second and the third peaks appear at systematically smaller r for samples recovered from higher pressures. It may be pointed out that the WO_4 tetrahedra and ZrO_6 octahedra are not regular even in the cubic phase due to lower site symmetries. The shortest bond in crystalline α-$Zr(WO_4)_2$ is the W-O bond and the bond length, averaged over all four distinct oxygen neighbors O_1 to O_4, is 1.767 Å. In addition, the average Zr-O distance in the cubic phase is 2.078 Å, only 0.3 Å longer than the W-O distance.[17] Although the amorphous phase is about 26% denser than the cubic phase, the fundamental bond distances such as W-O and Zr-O are not expected to be drastically different from those in the crystalline phase. Of course, these bond distances could increase slightly if the oxygen coordination number of W and Zr go up. In view of this it is likely that the first peak that extends up to 2.3 Å could include both W-O and Zr-O coordinations. Since the ZrO_6 octahedra are less strongly bound than the WO_4 tetrahedra, one can expect ZrO_6 octahedra to compress and overlap with the W-O peak. It may be pointed out that only the neutron-weighted pair distribution function of 4 GPa-treated sample[28] shows separate peaks for Zr-O and W-O correlations. This arises due to large neutron weights to correlations involving oxygen. On the other hand, because of small x-ray weights for zirconium and oxygen, in the x-ray-weighted $g(r)$ the Zr-O correlations appear only as small shoulder riding on the first peak.[28] It is worth comparing the $g(r)$ reported for 4 GPa sample obtained using the $S(q)$ data up to 15 $Å^{-1}$ with that for the 5.5 GPa sample (Fig. 4) obtained using the $S(q)$ data up to 8 $Å^{-1}$. It is found that the asymmetry of the first peak and the weak sharp feature at 3.25 Å are not noticeable in the present work; however, the first peak in the two cases has nearly the same width. This suggests that the broad nature of the peaks is predominantly due to the amorphous structure and partly due to lower resolution. On the other hand, for crystalline solids, it is essential to measure data typically up to 25 $Å^{-1}$ to get a good $g(r)$.

The second peak in $g(r)$ appears at 2.77 Å in 5.5 GPa-treated sample. This peak has been attributed to O-O distance on the basis of reverse Monte Carlo (RMC) simulation[28] on densified crystal-based model for a-$Zr(WO_4)_2$ that constrained the coordination for W to be 5. In the cubic phase, O-O distance occurs at 2.9 Å.[28] Short O-O distance in the amorphous phase suggests that the open network of the crystal is indeed compressed to allow closer O-O contacts both within and between polyhedra. The center of the second peak shows a systematic shift to lower r at higher pressures. This suggests that the oxygen atoms move even closer in the samples recovered from higher pressures. An increase in the height of the second peak suggests a growth of the O-O correlations at high pressure.

The third peak occurs at 3.72 Å in 5.5 GPa-treated sample and it corresponds to both W-W and W-Zr distances. In the cubic phase, W-Zr and W-W distances are 3.82 Å and 4.11 Å respectively.[17] Significantly shorter distance in the amorphous phase as compared to that in the crystal essentially represents collapse of corner-linked network structure resulting in densification. This peak also shifts inward at higher pressures. Shift of this peak to shorter r also suggests further densification at high pressures. The small shifts of the different neighbor distances to lower r suggesting monotonic densification is consistent with the shift of the first peak of $S(q)$. Figure 5 shows the dependence of the positions of the peaks in $g(r)$ as a function of soaking pressure. One can see that the second and the third neighbor shells are much smaller in radius than the corresponding O-O and the W-W and W-Zr distances in the cubic phase suggesting that the densification occurs via reduction in these nonbonding distances. It may be pointed out that Zr-Zr distance in the cubic phase (specific volume 192 $Å^3$) appears at 6.4 Å. In order to account for reduced specific volume of 153 $Å^3$, a value of 6 Å was used for the Zr-Zr distance in a disordered crystal-based RMC simulation[28] of 4 GPa-treated amorphous sample, where Zr-sublattice remained crystalline. On the other hand, in the $g(r)$'s for the present 5.5 GPa-treated sample as well as in that reported for 4 GPa sample,[28] no prominent features corresponding to Zr-Zr correlations are found. This is because of small weight factors of Zr-Zr partial pair correlations for the neutron as well as the x-ray diffraction, and hence the RMC simulation with a crystalline Zr-sublattice could reproduce the data.

As discussed in Sec. I, in the amorphous $Zr(WO_4)_2$, there are several possibilities about the coordination numbers of W such as 5,[28] 6,[26] and 7.[31] Similarly a coordination of 7 has been found for Zr also.[32] Distortions and relative tilts of

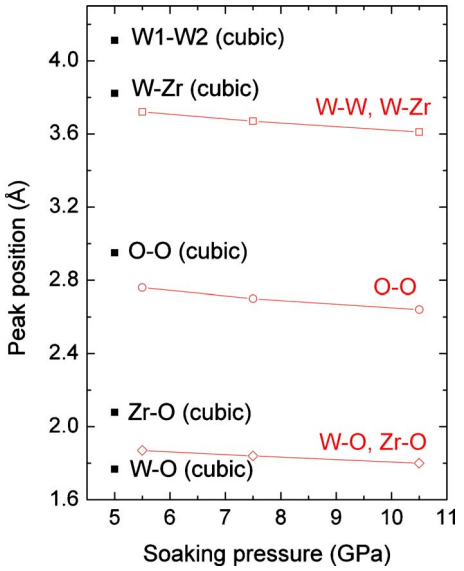

FIG. 5. (Color online) Dependence of the first three peaks in the pair-correlation function $g(r)$ as a function of soaking pressure. Filled symbols at 5 GPa are the bond distances in the ambient pressure cubic phase for comparison.

octahedra with respect to those of the tetrahedra can cause O-O distance to reduce. This can bring oxygen of one WO_4 in the neighborhood of another ZrO_6 and vice versa and eventually result in higher coordination for W and Zr. Such tilts would also transform corner-sharing polyhedra to edge-sharing first and to face-sharing next thereby reducing the empty spaces in between the distorted polyhedra leading to gradually denser random polyhedral packing. Hence as pressure is increased, a gradual increase in the number of edge- and face-sharing polyhedra at random locations in the structure could occur. Thus it is, in principle, possible to have amorphous phases distinct in terms of coordination number and local topology. We now examine the present results in the context of possible increase in coordination number within the amorphous phase and consequent polyamorphism. One can see from Fig. 4 that the first peak broadens and its height reduces at 10.5 GPa. The integrated intensity for this peak is a weighted average of the number of bonds for W-O and Zr-O nearest-neighbor pairs. We find that the integrated intensity marginally reduces. This implies that the coordination number essentially remains unchanged within the amorphous phase. Furthermore, monotonic changes in the neighbor distances rules out the possibility of distinct amorphous phases.

V. CONCLUSIONS

Structure of pressure-amorphized $Zr(WO_4)_2$ is investigated using synchrotron x-ray diffraction. Structure factors $S(q)$ of samples recovered from different pressures are obtained after applying corrections for air-scattering and angle-dependent attenuation correction to the data. The first peak in the structure factor of 5.5 GPa-treated sample is found to occur at a lower q than those recovered from higher pressures. The pair-correlation functions $g(r)$, obtained by Fourier transforming $S(q)$, suggests that further densification of amorphous phase occurs via contraction of second and third neighbor shells representing O-O and W-W and W-Zr distances, respectively, rather than first neighbor shell. Furthermore, there is no evidence of increase in coordination number in the recovered samples and consequent polyamorphism.

ACKNOWLEDGMENTS

It is a pleasure to thank T. A. Mary for the samples, T. R. Ravindran for pressure treating the samples in a diamond-anvil cell, and V. S. Sastry for many helpful discussions. A.K.A. thanks C. S. Sundar for interest in the work and Baldev Raj for support and encouragement.

*Corresponding author. aka@igcar.gov.in

[1] A. L. Goodwin, M. Calleja, M. J. Conterio, M. T. Dove, J. S. O. Evans, D. A. Keen, L. Peters, and M. G. Tucker, Science **319**, 794 (2008).
[2] D. J. Williams, D. E. Partin, F. J. Lincoln, J. Kouvetakis, and M. O'Keefe, J. Solid State Chem. **134**, 164 (1997).
[3] J. S. O. Evans, T. A. Mary, T. Vogt, M. A. Subramanian, and A. W. Sleight, Chem. Mater. **8**, 2809 (1996).
[4] G. D. Barrera, J. A. O. Bruno, T. H. K. Barron, and N. L. Allan, J. Phys.: Condens. Matter **17**, R217 (2005).
[5] T. R. Ravindran and A. K. Arora, Phys. Rev. Lett. **86**, 4977 (2001).
[6] A. K. Arora, T. R. Ravindran, and S. Chandra, J. Phys.: Condens. Matter **19**, 226210 (2007).
[7] T. R. Ravindran, A. K. Arora, S. Chandra, M. C. Valsakumar, and N. V. C. Shekar, Phys. Rev. B **76**, 054302 (2007).
[8] X. Yang, X. Cheng, X. Yan, J. Yang, T. Fu, and J. Qui, Compos. Sci. Technol. **67**, 1167 (2007).
[9] V. Sivasubramanian, T. R. Ravindran, S. Kalavathi, and A. K. Arora, J. Electroceram. **17**, 57 (2006).
[10] N. Khosrovani, A. W. Sleight, and T. Vogt, J. Solid State Chem. **132**, 355 (1997).
[11] T. R. Ravindran, A. K. Arora, and T. A. Mary, Phys. Rev. Lett. **84**, 3879 (2000).
[12] D. Cao, F. Bridges, G. R. Kowach, and A. P. Ramirez, Phys. Rev. B **68**, 014303 (2003).
[13] R. Mittal, S. L. Chaplot, A. I. Kolesnikov, C. K. Loong, and T. A. Mary, Phys. Rev. B **68**, 054302 (2003).
[14] J. N. Hancock, C. Turpen, Z. Schlesinger, G. R. Kowach, and A. P. Ramirez, Phys. Rev. Lett. **93**, 225501 (2004).
[15] C. A. Kennedy and M. A. White, Solid State Commun. **134**, 271 (2005).
[16] F. R. Drymiotis, H. Ledbetter, J. B. Betts, T. Kimura, J. C. Lashley, A. Migliori, A. P. Ramirez, G. R. Kowach, and J. V. Duijn, Phys. Rev. Lett. **93**, 025502 (2004).
[17] M. G. Tucker, A. L. Goodwin, M. T. Dove, D. A. Keen, S. A.

Wells, and J. S. O. Evans, Phys. Rev. Lett. **95**, 255501 (2005).
[18] Z. Schlesinger, J. A. Rosen, J. N. Hancock, and A. P. Ramirez, Phys. Rev. Lett. **101**, 015501 (2008).
[19] T. R. Ravindran, A. K. Arora, and T. A. Mary, Phys. Rev. B **67**, 064301 (2003).
[20] R. Govindaraj, C. S. Sundar, and A. K. Arora, Phys. Rev. B **76**, 012104 (2007).
[21] J. D. Jorgensen, Z. Hu, S. Teslic, D. N. Argyriou, S. Short, J. S. O. Evans, and A. W. Slight, Phys. Rev. B **59**, 215 (1999).
[22] T. R. Ravindran, A. K. Arora, and T. A. Mary, J. Phys.: Condens. Matter **13**, 11573 (2001).
[23] C. A. Perottoni, J. E. Zorzi, and J. H. A. da Jornada, Solid State Commun. **134**, 319 (2005).
[24] A. K. Arora, R. Nithya, T. Yagi, N. Miyajima, and T. A. Mary, Solid State Commun. **129**, 9 (2004).
[25] T. Sakuntala, A. K. Arora, V. Sivasubramanian, R. Rao, S. Kalavathy, and S. K. Deb, Phys. Rev. B **75**, 174119 (2007).
[26] A. K. Arora, V. S. Sastry, P. Ch. Sahu, and T. A. Mary, J. Phys.: Condens. Matter **16**, 1025 (2004).
[27] J. Catafesta, J. E. Zorzi, C. A. Perottoni, M. R. Gallas, and J. A. H. da Jornada, J. Am. Ceram. Soc. **89**, 2341 (2006).
[28] D. A. Keen, A. W. Goodwin, M. G. Tucker, M. T. Dove, J. S. O. Evans, W. A. Crichton, and M. Brunelli, Phys. Rev. Lett. **98**, 225501 (2007).
[29] W. Liu and B. Li, Appl. Phys. Lett. **93**, 191904 (2008).
[30] J. M. Gallardo-Amores, U. Amador, E. Moran, and M. A. A. Franco, Int. J. Inorg. Mater. **2**, 123 (2000).
[31] A. Grzechnik, W. A. Crichton, A. Syassen, P. Adler, and M. Mezouar, Chem. Mater. **13**, 4255 (2001).
[32] T. Varga and A. P. Wilkinson, Phys. Rev. B **79**, 224119 (2009).
[33] T. R. Ravindran, A. K. Arora, V. S. Sastry, and P. C. Sahu, J. Non-Cryst. Solids **355**, 2289 (2009).
[34] P. H. Poole, T. Grande, C. A. Angell, and P. F. McMillan, Science **275**, 322 (1997).
[35] O. Mishima, L. D. Calvert, and E. Whalley, Nature (London) **314**, 76 (1985).
[36] D. J. Lacks, Phys. Rev. Lett. **84**, 4629 (2000).
[37] G. D. Mukherjee, S. N. Vaidya, and V. Sugandhi, Phys. Rev. Lett. **87**, 195501 (2001).
[38] J. Krogh-Moe, Acta Crystallogr. **9**, 951 (1956).
[39] V. H. Smith, Jr., A. J. Thakkar, and D. C. Chapman, Acta Crystallogr., Sect. A: Cryst. Phys., Diffr., Theor. Gen. Crystallogr. **31**, 391 (1975).
[40] *International Tables for X-ray Crystallography* (The Kynoch Press, Birmingham, 1974), Vol. IV, p. 71.
[41] A. C. Geiculescu and H. J. Rack, J. Sol-Gel Sci. Technol. **20**, 13 (2001).
[42] R. Kesavamoorthy, B. V. R. Tata, A. K. Arora, and A. K. Sood, Phys. Lett. A **138**, 208 (1989).
[43] J. P. Hansen and L. Verlet, Phys. Rev. **184**, 151 (1969).
[44] D. Daisenberger, M. Wilson, P. F. McMillan, R. Q. Cabrera, M. C. Wilding, and D. Machon, Phys. Rev. B **75**, 224118 (2007).
[45] R. Kesavamoorthy and A. K. Arora, J. Phys. A **18**, 3389 (1985).